

# Proteasome inhibitor PS-341 (VELCADE) induces stabilization of the TRAIL receptor DR5 mRNA through the 3'-untranslated region

Karthikeyan Kandasamy and Andrew S. Kraft

Hollings Cancer Center, Medical University of South Carolina, Charleston, South Carolina

## Abstract

Addition of proteasome inhibitor PS-341 (VELCADE, bortezomib) to prostate cancer cells enhances cell death mediated by tumor necrosis factor-related apoptosis-inducing ligand (TRAIL). PS-341 sensitizes prostate cancer cells to TRAIL-induced apoptosis by increasing TRAIL receptors (DR5), inhibiting protein degradation, and elevating DR5 mRNA. Investigations into how PS-341 regulates the stability of DR5 mRNA revealed that PS-341 increased DR5 mRNA by extending its half-life from 4 to 10 h. The 2.5-kb 3'-untranslated region of the DR5 gene stabilized a heterologous gene in LNCaP human prostate cancer cells, suggesting the importance of this mRNA sequence. In contrast, human prostate cancer cell lines PC-3 and DU145 do not show this stabilization, suggesting cell specificity. PS-341 treatment of LNCaP cells increases the level of specific cytoplasmic mRNA-binding proteins, including AUF-1 isoforms, hnRNP C1/C2, and HuR proteins. In UV cross-linking experiments, after PS-341 treatment, the HuR protein markedly increases binding to specific sequences in the DR5 3'-untranslated region. In LNCaP cells treated with PS-341, small interfering RNA-mediated knockdown of HuR markedly decreases the half-life of DR5 mRNA, indicating that HuR is essential for mRNA stabilization. HuR protein is ubiquitinated, suggesting that PS-341 increases this protein by preventing its degradation. These experiments implicate modulation of mRNA stability as a novel mechanism by which proteasome inhibitors function, sensitizing cancer cells to antineoplastic agents. [Mol Cancer Ther 2008;7(5):1091–100]

## Introduction

Tumor necrosis factor-related apoptosis-inducing ligand (TRAIL) is a proapoptotic protein thought to be a potential anticancer agent due to its ability to target tumor but not normal cells and its *in vivo* activity against a wide range of tumor types including melanoma, breast, and prostate cancer (for reviews, see refs. 1–3). Cytotoxic agonist antibodies directed against TRAIL receptors have been developed and are useful against multiple tumor types (4–6) and these antibodies have entered clinical trials. The proteasome inhibitor PS-341 (VELCADE, bortezomib; ref. 7) has been shown to greatly enhance the killing activity of TRAIL (8–11) by increasing TRAIL receptors, DR4 (TRAIL R1) and DR5 (TRAIL R2; ref. 12). This increase in TRAIL receptors occurs via the inhibition of ubiquitinated TRAIL receptor degradation and by increasing TRAIL receptor mRNA (12). In both yeast and multiple myeloma cells in culture (13, 14), the addition of PS-341 both increases and decreases specific mRNAs, suggesting that regulation of gene transcription by this agent is a general phenomenon not limited to the TRAIL receptor or prostate cancer cells.

The mechanism by which PS-341 controls the transcription of DR5 is complex, but in multiple myeloma and head and neck cancer cells, the unfolded protein response is involved (15–17). PS-341 induces PERK, an ER stress-specific eIF-2 $\alpha$  kinase, ATF4, an ER stress-induced transcription factor, and its proapoptotic target CHOP/GADD153 (15–17). Because the DR5 upstream region contains a CHOP-binding sequence, induction of these proteins can stimulate the transcription of this gene (18, 19). In addition to the CHOP binding site, the first intron of the DR5 gene contains binding sites for both p53 and nuclear factor- $\kappa$ B: DR5 was first cloned as a p53-responsive gene (20, 21), and regulation of nuclear factor- $\kappa$ B activity can modulate the transcription of this gene (22). The transcriptional regulation of DR5 is complex, and mapping the promoter region reveals multiple potential transcription factor binding sites.

An alternative to transcriptional control mechanisms for modulating DR5 levels is mRNA stability regulation. Many inflammatory mediators, growth factors, and cytokines, such as tumor necrosis factor- $\alpha$ , interleukin-1 $\beta$ , interleukin-8, granulocyte macrophage colony-stimulating factor, macrophage inflammatory protein 1 $\alpha$ , and vascular endothelial growth factor, are all regulated by mRNA stability (23–28). These mRNAs contain class II AU-rich elements found in the 3'-untranslated region (UTR) that bind protein factors, which regulate mRNA half-life. In addition, there are AU-rich elements (class I) that are mostly found in the 3'-UTR of proto-oncogenes, e.g., c-Fos (29). Proteins that

Received 12/5/07; revised 2/20/08; accepted 2/25/08.

Grant support: NIH grant R01 CA104710 (A.S. Kraft).

The costs of publication of this article were defrayed in part by the payment of page charges. This article must therefore be hereby marked *advertisement* in accordance with 18 U.S.C. Section 1734 solely to indicate this fact.

Requests for reprints: Andrew S. Kraft, Hollings Cancer Center, Medical University of South Carolina, 86 Jonathan Lucas Street, Suite 124, Charleston, SC 29425. Phone: 843-792-8284; Fax: 843-792-9456. E-mail: Kraft@musc.edu

Copyright © 2008 American Association for Cancer Research.

doi:10.1158/1535-7163.MCT-07-2368

can directly bind to AU-rich elements to promote mRNA decay include tristetraprolin (30, 31), BRF1 (32), and TIA-1 (33), whereas mRNA-stabilizing proteins include the AUF-1 isoforms and the HuR protein (34–36). The levels and activity of these mRNA-binding proteins can be regulated both transcriptionally and post-translationally.

To further understand how PS-341 increases DR5, we investigated whether PS-341 treatment increases the stability of DR5 mRNA. This potential mechanism is suggested by the observation that the DR5 3'-UTR contains several AU-rich regions capable of binding proteins that post-transcriptionally regulate this mRNA (37). We find that PS-341 treatment increases the stability of DR5 mRNA half-life from 4 to 10 h, enhances the binding of cytoplasmic proteins to the DR5 3'-UTR mRNA, and increases cytoplasmic levels of mRNA-binding proteins.

## Materials and Methods

### Cell Culture and Reagents

LNCaP, PC-3, and DU145 prostate cancer cell lines were purchased from American Type Culture Collection. LNCaP cells were cultured in RPMI 1640, and PC-3 and DU145 cells were cultured in DMEM (Hyclone) supplemented with 10% fetal bovine serum (Hyclone) and 100 µg/mL penicillin-streptomycin (Invitrogen). Cells were grown in 5% CO<sub>2</sub> at 37°C. Antibodies used for Western blot analysis at a dilution of 1:1,000 include a HuR monoclonal antibody (3A2), TIAR, TIA-1, tristetraprolin, hnRNP C1/C2, glyceraldehyde-3-phosphate dehydrogenase (GAPDH), and Lamin B1 all purchased from Santa Cruz Biotechnology. A TIAR monoclonal antibody used for immunoprecipitation was purchased from BD Biosciences. The AUF-1 antibody (1:4,000 dilution) was obtained from Upstate Biotechnology. The anti-HA antibody was obtained from Covance. Anti-Flag M2 antibody, anti-Flag beads, and anti-HA beads were from Sigma. Protein A agarose beads were supplied by Invitrogen. All secondary antibodies conjugated to horseradish peroxidase were from Amersham Biosciences and diluted 1:5,000. The riboprobe *in vitro* transcription kit was purchased from Promega. All other chemicals were purchased from Sigma, unless otherwise indicated.

### Plasmid Constructs and Transfection

A full-length DR5 clone was obtained from Origene. Using this clone as a template, DR5 3'-UTR fragments were generated by PCR amplification (see Supplementary Table S1 for oligomers)<sup>1</sup> and cloned into a pSP70 vector (Promega). For reporter plasmid construction, the DR5 coding region was replaced with the enhanced green fluorescent protein (EGFP) coding region amplified from pIRES2-EGFP (Clontech).

For mRNA stability experiments, 24 h after transfection, LNCaP cells were treated with DMSO or PS-341 (0.5 µmol/L,

12 h) followed by actinomycin D (2 µg/mL), and cells were harvested for mRNA quantification. For analysis of small interfering RNA (siRNA) duplex effects and EGFP reporter expression 24 h after electroporation, cells were treated with PS-341 (0.1 µmol/L) for 12 h followed by the addition of actinomycin D (2 µg/mL). The cells were then harvested at regular time intervals for mRNA measurements. For protein analysis in cytoplasmic extracts, siRNA duplex transfected cells were harvested after 36 h of electroporation. All of the siRNA duplexes (see Supplementary Table S1)<sup>1</sup> were obtained from Dharmacon.

For transfection of cDNA into LNCaP cells,  $1.0 \times 10^7$  cells/mL were electroporated at 280 mV and 950 µF using a Bio-Rad Gene Pulser II System. Alternatively, LipofectAMINE (Invitrogen) was also used for transfection. For the assessment of cell viability, scrambled or HuR siRNA-transfected cells were plated onto a 96-well plate. Twenty-four hours after transfection, the cells were treated with PS-341, TRAIL, or the combination for 18 h and cell viability measured by the MTS assay (38).

### Preparation of Protein Extracts followed by Western Blotting

Cytoplasmic extracts were prepared from the pelleted cells by hypotonic lysis buffer following the protocol as reported by Ford et al. (39). Nuclei were pelleted, and the protein was extracted with nuclear extraction buffer [10 mmol/L HEPES (pH 7.9), 0.41 mol/L KCl, 1.5 mmol/L MgCl<sub>2</sub>, 0.5 mmol/L DTT, 25% glycerol, 0.2 mmol/L EDTA, 0.1 mmol/L phenylmethylsulfonyl fluoride (PMSF)], and the extract was centrifuged at 14,000 rpm for 10 min. For other Western blotting experiments, the pelleted cells were lysed in a buffer containing 20 mmol/L Tris-HCl (pH 7.4), 150 mmol/L NaCl, 2 mmol/L EDTA, 10% glycerol, 1% Triton X-100, 1 mmol/L PMSF, and protease inhibitor cocktail. The lysates were cleared by centrifugation at 14,000 rpm for 15 min and the supernatant was stored at -80°C. Total protein (30 µg) was resolved by 12% SDS-PAGE and transferred to polyvinylidene difluoride membrane followed by blocking in 3% bovine serum albumin.

### RNase Protection Assays

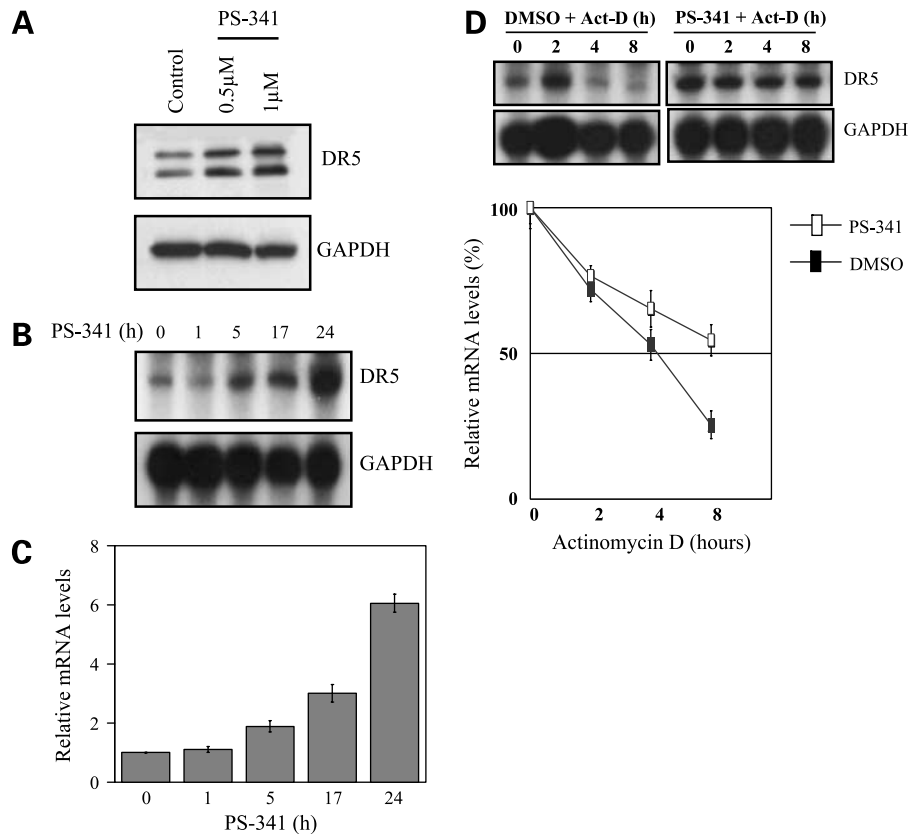
RNase protection assays were done according to the Riboquant protocol described by BD PharMingen. For RNase protection assays, the DR5 probe was PCR amplified from the full-length clone, whereas the GAPDH probe was amplified from the LNCaP cDNA prepared for real-time PCR. Both probes were cloned into a pSP70 vector (Promega).

### UV Cross-Linking and Label Transfer Assay

For UV cross-linking experiments, an aliquot of radio-labeled transcript ( $1 \times 10^6$  counts/min) and yeast RNA (10 µg) with or without competing unlabeled RNA transcripts used at the indicated molar excess were added to the mixture containing LNCaP cytoplasmic extract (50 µg), 15 mmol/L HEPES (pH 7.6), 40 mmol/L KCl, 5 mmol/L MgCl<sub>2</sub>, 1% glycerol, yeast RNA (10 µg), heparin (10 µg), and 65 units RNasin in a total volume of 50 µL. Mixtures were incubated for 10 min at 22°C and exposed to short-wave (254 nm) UV irradiation at a distance of 7 cm for 30 min.

<sup>1</sup> Supplementary materials for this article are available at Molecular Cancer Therapeutics Online (<http://mct.aacrjournals.org/>).

**Figure 1.** Regulation of DR5 mRNA stability by PS-341 in LNCaP cells. **A**, Western blot analysis of DR5 and GAPDH in extracts prepared from LNCaP cells treated with PS-341 for 18 h. **B**, autoradiographic images of RNase protection assays done on samples prepared from LNCaP cells treated with PS-341 (500 nmol/L) for indicated times. After treatment, total RNA was isolated using TRIzol, and equal quantities of RNA were used for assaying DR5 mRNA and GAPDH mRNA using specific probes. **C**, quantitative real-time PCR analysis of DR5 mRNA in LNCaP samples in **B** normalized to endogenous GAPDH mRNA and plotted as fold increase in mRNA. This experiment was repeated in triplicate and the mean  $\pm$  SD is plotted. **D**, autoradiographic images of RNase protection assay done on the samples from LNCaP were treated with either DMSO or PS-341 (0.5  $\mu$ mol/L, 12 h), followed by treatment with actinomycin D (2  $\mu$ g/mL). After treatment with actinomycin D, cells were harvested at various times for RNA and the RNase protection assays were done for DR5 and GAPDH. Quantitative real-time PCR analysis done on the LNCaP samples shown in this figure normalized to GAPDH levels. Experiments were repeated in triplicate and the mean  $\pm$  SD is shown.



Transcripts that were not cross-linked to protein were digested with RNase A (0.5 mg/mL) and RNase T1 (10 units/mL) at 37°C for 30 min. For immunoprecipitation of proteins bound to radiolabeled transcripts, after treatment with RNases, the mixtures were incubated with protein A-agarose beads (Invitrogen) precoated with 1  $\mu$ g HuR (Santa Cruz Biotechnology), TIAR (BD PharMingen), or nonspecific IgG antibodies overnight at 4°C. The beads were washed with NT2 buffer (40) six times and resolved in 10% SDS-PAGE, dried, and subjected to autoradiography and phosphorimaging for quantitation.

#### Immunoprecipitation of Endogenous RNA-Protein Complexes

Immunoprecipitation of endogenous RNA-protein complexes were done according to the method of Tenenbaum et al. (40). LNCaP cytoplasmic extracts (200  $\mu$ g) were incubated (overnight at 4°C) with protein A-agarose beads (Invitrogen), which were precoated with 2  $\mu$ g HuR, TIA-1, TIAR, and hnRNP C1/C2 antibodies (Santa Cruz Biotechnology) and AUF-1 antibodies (Upstate Biotechnology) in a mixture containing 50 mmol/L Tris-HCl (pH 7.4), 150 mmol/L NaCl, 1 mmol/L MgCl<sub>2</sub>, 0.05% NP-40, 15 mmol/L EDTA, 1 mmol/L DTT, 10 mg/mL yeast RNA, 1 mg/mL heparin, and 65 units RNasin. After incubation, the beads were washed six times with NT2 buffer [50 mmol/L Tris-HCl (pH 7.4), 150 mmol/L NaCl, 1 mmol/L MgCl<sub>2</sub>, 0.05% NP-40] and further incubated with 100  $\mu$ L NT2 buffer

containing 0.1% SDS and 0.5 mg/mL proteinase K (30 min, 50°C). The RNA was extracted from these immunoprecipitates using TRIzol-containing glycoblue (Ambion) as a coprecipitant and was quantitated by PCR.

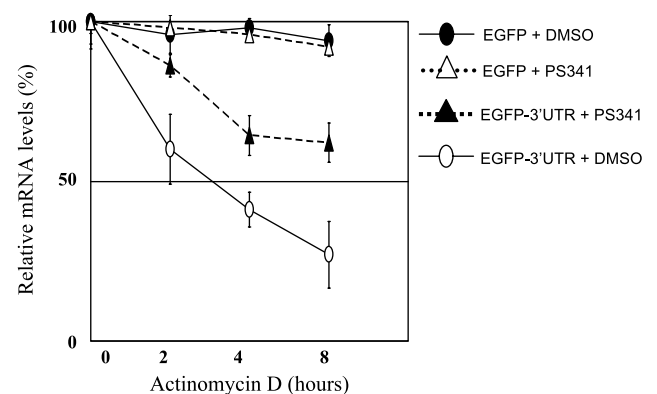


**Figure 2.** PS-341 treatment stabilizes reporter EGFP transcripts in the presence of the 3'-UTR of DR5. LNCaP cells were transfected with EGFP plasmid alone or EGFP plasmid containing 3'-UTR of DR5. Twenty-four hours after transfection, LNCaP cells were treated with DMSO (0.05%) or PS-341 (500 nmol/L) for 14 h. Transfected cells were then washed with PBS, treated with actinomycin D (2  $\mu$ g/mL), and then harvested for RNA isolation at 0, 2, 4, and 8 h. EGFP was measured by quantitative real-time PCR analysis and the values were normalized to cotransfected rat GAPDH levels. Experiments were repeated in triplicate and the mean  $\pm$  SD is plotted.

### Real-time Reverse Transcription PCR

For real-time reverse transcription-PCR, RNA isolated from the immunoprecipitation samples was reverse transcribed using random hexamers and SuperScript II RT (Invitrogen) and the resulting cDNA was used for PCR amplification using gene-specific primer pairs. Quantitative PCR conditions for these reactions were as follows: 95°C for 10 s, 58°C for 30 s, and 72°C 10 s for 40 cycles.

### Nonquantitative PCR

PCR was carried out for Fig. 6A in the immunoprecipitated samples under the following conditions: 94°C for 30 s, 50°C for 45 s, and 68°C for 45 s for 25 cycles and the resulting product was separated with 1% agarose gel electrophoresis.

## Results

### PS-341 Treatment Increases DR5 in LNCaP Cells

In LNCaP prostate cancer cells, proteasomal inhibition by PS-341 for 18 h induced a 3-fold increase in DR5 protein levels (Fig. 1A). To examine whether the protein increase is secondary to DR5 mRNA accumulation in LNCaP cells, we measured DR5 mRNA after PS-341 treatment using a RNase protection assay (Fig. 1B). To measure this increase, quantitative real-time PCR was done (Fig. 1C). Results indicate that mRNA levels increased after 5 h of PS-341 treatment, and by 24 h, a 6-fold increase was evident. Results observed in these experiments with PS-341 were identical to those obtained with the proteasome inhibitor MG-132 (data not shown). Because the DR5 gene has a long

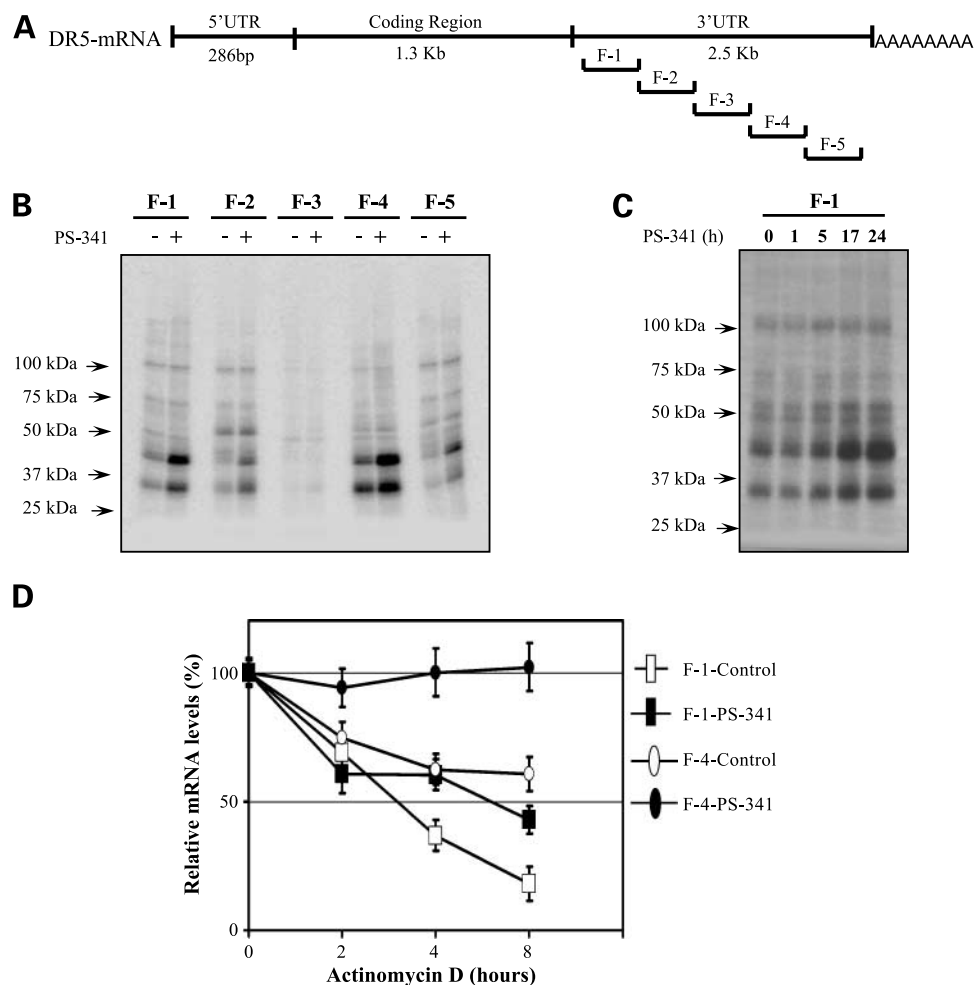


**Figure 3.** PS-341 treatment increases the binding of proteins to the fragments of the 3'-UTR. **A**, schematic representation of the DR5 mRNA and the fragments of 3'-UTR. **B**, autoradiographic images of the RNA-protein interactions shown by UV cross-linking experiments. Fifty micrograms of cytoplasmic extracts from LNCaP cells treated with or without PS-341 (500 nmol/L, 18 h) were incubated with *in vitro* transcribed, radiolabeled F-1, F-2, F-3, F-4, and F-5 transcripts and UV cross-linked for 30 min. Excess RNA was digested with RNase cocktail and the cross-linked proteins were resolved via 10% SDS-PAGE. The gel was dried and subjected to autoradiography. **C**, time course of binding of PS-341-induced proteins to the F-1 fragment. Experiment was carried out as in **B** using cytoplasmic extracts from LNCaP cells at varying times after PS-341 treatment. **D**, stabilization of EGFP mRNA by the 3'-UTR fragments F-1 and F-4. The experiment was carried out identically to Fig. 2, except that only a portion of the 3'-UTR of DR5 was cloned after the EGFP reporter.

3'-UTR, we hypothesized that the mRNA may be post-transcriptionally regulated. To examine this possibility, we measured mRNA half-life after actinomycin D treatment. PS-341 and actinomycin D concentrations were carefully selected to avoid synergistic toxicity induced by the use of these agents. LNCaP cells were treated with PS-341 (500 nmol/L) for 12 h followed by actinomycin D (2  $\mu$ g/mL). These experiments reveal that DR5 mRNA half-life is ~4 h in LNCaP cells, whereas the half-life of DR5 mRNA after PS-341 treatment is dramatically increased to at least 8 h by RNase protection assay and quantitative PCR (Fig. 1D). We next evaluated DU145 and PC-3 cells and found that PS-341 treatment increased DR5 mRNA in the human prostate cancer cell line, DU145, but did not stabilize mRNA (data not shown; Supplementary Fig. S1A).<sup>1</sup> Variability in the 4- and 8-h time points can be accounted for by the difference in loading that is seen with the GAPDH control (Supplementary Fig. S1A).<sup>1</sup> Treatment of PC-3 cells with this compound neither stabilized DR5 mRNA nor increased its half-life (Supplementary Fig. S1A).<sup>1</sup> Although the cell lines were human prostate cancer cells, results suggest that the ability of this compound to regulate mRNA stability is cell type specific.

#### PS-341 Stabilizes a Heterologous Reporter Gene

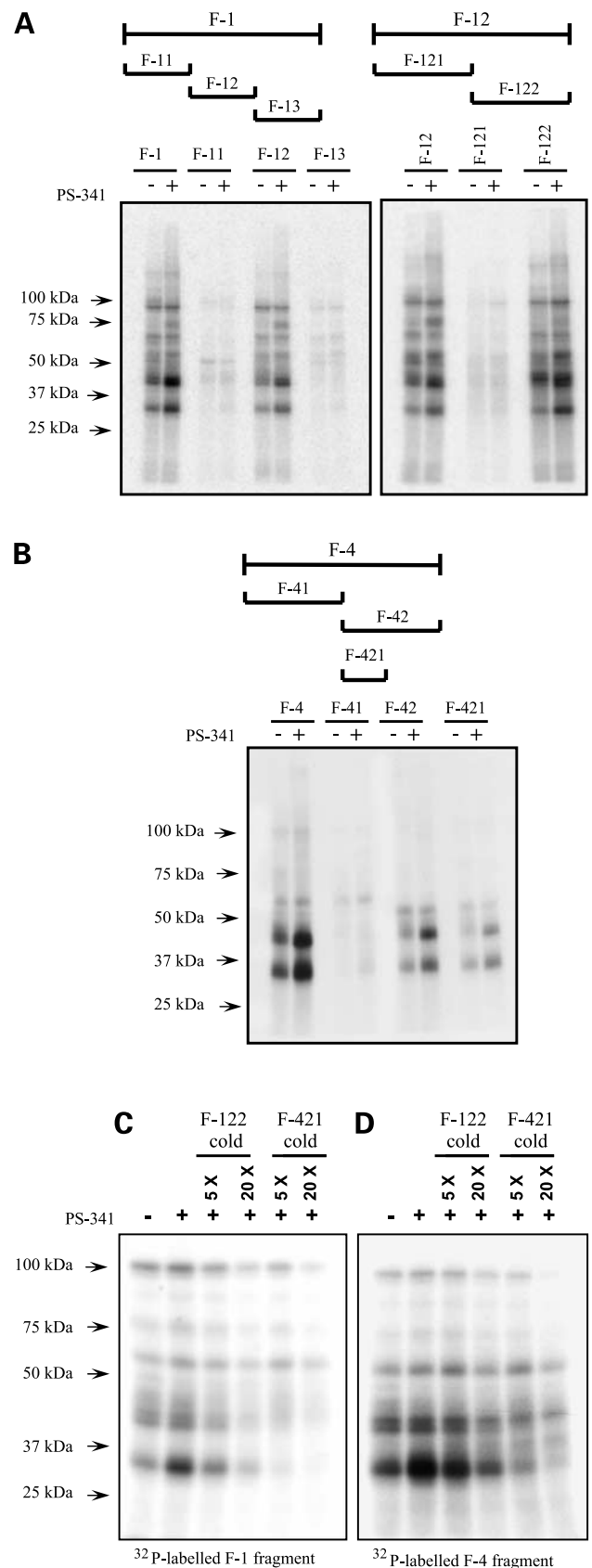
To examine whether the 3'-UTR of DR5 has a general effect on the stability of other genes, we cloned the EGFP coding region into the pcDNA3.1 vector followed by the 3'-UTR of the DR5 mRNA (Fig. 2). LNCaP cells were transiently transfected with EGFP plasmid alone or with an EGFP-3'-UTR plasmid. Figure 2 shows that PS-341 treatment stabilized EGFP-3'-UTR mRNA with a messenger half-life of >8 h, whereas in DMSO treated cells the half-life was between 3 and 4 h. In comparison with the half-life of the EGFP-3'-UTR mRNA, the EGFP message that did not contain the UTR was not different in control or PS-341-treated LNCaP cells. Thus, the 3'-UTR of DR5 mRNA likely contains regulatory sequences that mediate the stability of this transcript after PS-341 treatment.

#### Identification of Regulatory Elements in DR5 3'-UTR

To examine PS-341-induced changes in protein binding to the 3'-UTR of DR5, ~450-bp fragments of the UTR were cloned into a pSP70 vector. These plasmids were used to generate a radiolabeled transcript for identifying proteins that could regulate mRNA stability (Fig. 3A).

The generated radiolabeled fragments were UV cross-linked after incubation with the cytoplasmic extract prepared from LNCaP cells treated with and without PS-341. After UV cross-linking, the unbound transcripts were digested with RNases, and the cross-linked material was

**Figure 4.** Identical proteins bind to the F-1 and F-4 fragments. **A**, analysis of the protein binding location in the F-1 fragment. Details of the experiment are identical to Fig. 3B, except for the use of varied portions of the F-1 fragment. **B**, identification of protein binding region in the F-4 fragment. The experiment shown was carried in an identical fashion to Fig. 3B, except that small portions of the F-4 fragment were examined. **C**, a UV cross-linking experiment done using F-1 and F-4 radioactive probes with cross-competition by a molar excess of cold F-122 or F-421 fragments. **D**, a similar experiment to that shown in **C**, except that the F-4 fragment was <sup>32</sup>P-labeled.



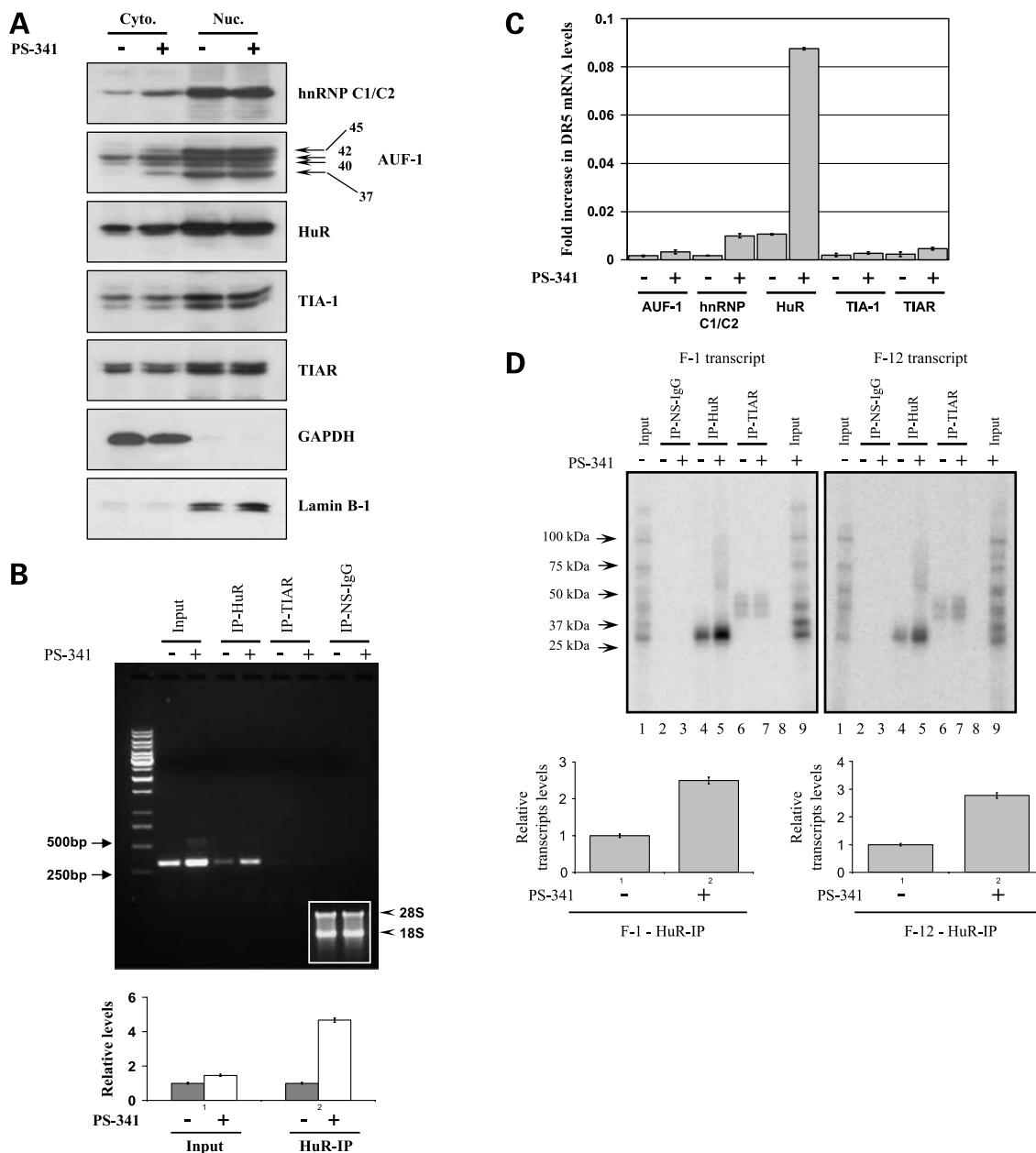


**Figure 5.** Analysis of RNA-binding proteins in LNCaP cells treated with PS-341. **A**, Western blot analysis of cytoplasmic (*Cyto*) and nuclear extracts (*Nuc*) prepared from vehicle or PS-341-treated (0.5  $\mu\text{mol/L}$ , 18 h) LNCaP cells. Cytoplasmic extracts (30  $\mu\text{g}$ ) and nuclear extracts (10  $\mu\text{g}$ ) were run on 12% SDS-PAGE, transferred to polyvinylidene difluoride membrane, and probed with antibodies to specific RNA-binding proteins. GAPDH was used as a loading control for the cytoplasmic extract, and Lamin B1 was a control for equivalent loading of nuclear proteins. **B**, PCR analysis of endogenous DR5 mRNA after immunoprecipitation of mRNA-binding proteins. Cytoplasmic extracts prepared from vehicle or PS-341-treated (500 nmol/L, 18 h) LNCaP cells were incubated with monoclonal HuR antibody, monoclonal TIAR antibody, or nonspecific IgG-coated protein A beads and immunoprecipitated in RNase-free conditions. RNA extracted from the immunoprecipitated complex was subjected to reverse transcription and PCR for 25 cycles. *Bottom*, bar graph of the relative RNA levels. Experiments were repeated in triplicate and the mean  $\pm$  SD is plotted. To establish equivalent levels of RNA in the samples, total RNA extracted from the cytoplasmic extracts was run on 1% formaldehyde agarose gel and ribosomal bands were photographed (see *inset*, lane 1 for vehicle and lane 2 for PS-341 treated). **C**, quantitative real-time PCR analysis of endogenous DR5 mRNA immunoprecipitated with various mRNA-binding proteins. The experiments were repeated in triplicate and the mean  $\pm$  SD is plotted. **D**, autoradiographic images of experiments carried out in a similar fashion to **B** using *in vitro* transcribed and radiolabeled F-1 and F-12 transcripts. LNCaP cells were treated with DMSO or PS-341 (500 nmol/L, 18 h) and UV cross-linked with F-1 and F-12 transcripts. RNA-binding proteins were immunoprecipitated with HuR or TIAR antibodies or nonspecific IgG. After immunoprecipitation, the complexes were separated via 10% SDS-PAGE and subjected to phosphorimaging. One tenth of the samples used for immunoprecipitation was loaded in lanes 1 and 9 without immunoprecipitation. *Bottom*, quantitative representation of the radioactivity in the transcripts immunoprecipitated with HuR antibody. The experiments were repeated in triplicate and the mean  $\pm$  SD is plotted.

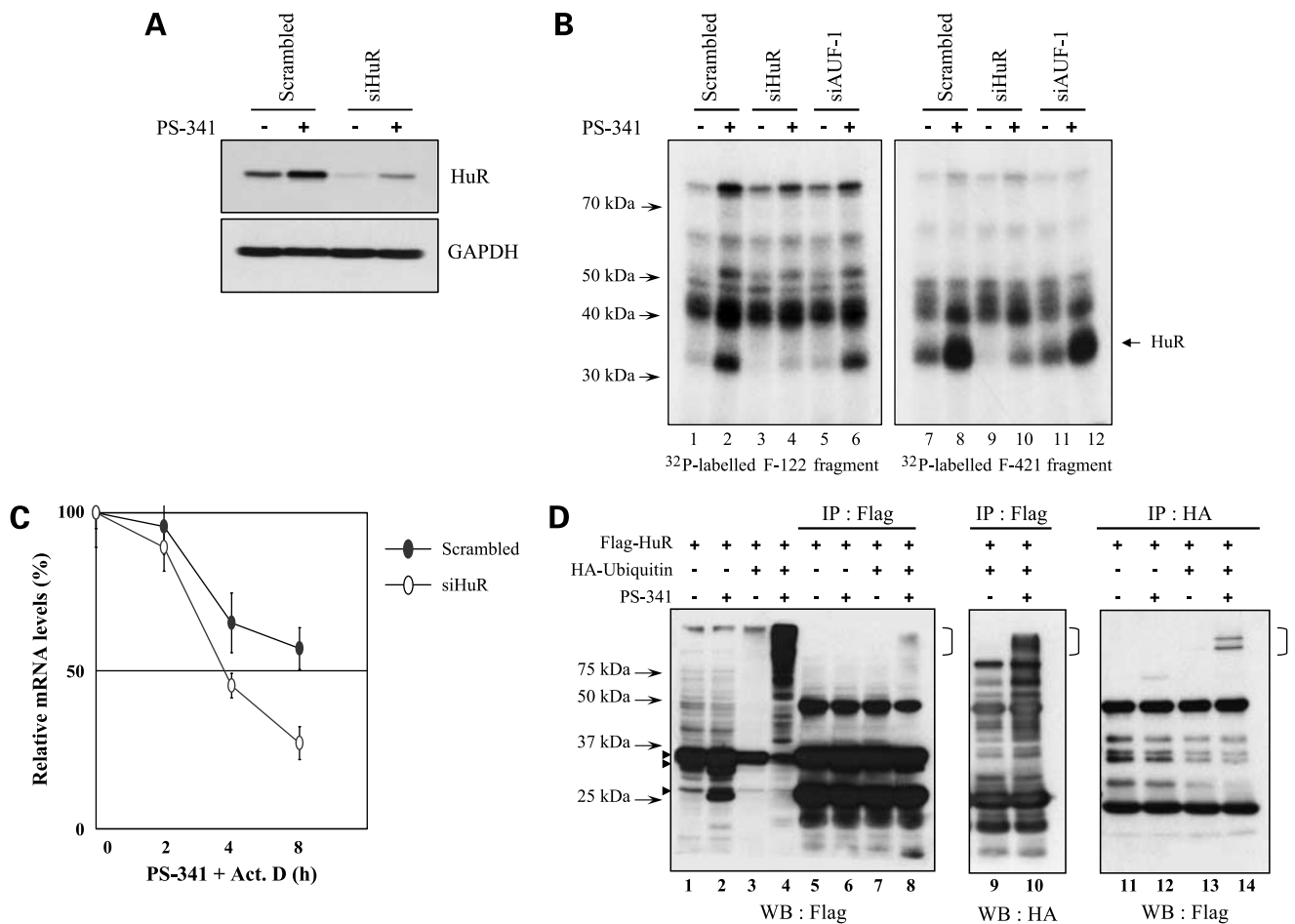


**Figure 6.** HuR stabilizes DR5 mRNA in LNCaP cells. **A**, Western blot analysis of samples from LNCaP cells transfected with scrambled or HuR siRNA. LNCaP cells ( $1 \times 10^7$ ) were electroporated with 150 pmol of either scrambled or HuR siRNA. Twenty-four hours after transfection, the cells were treated with PS-341 (500 nmol/L, 16 h) and the harvested cytoplasmic proteins were subjected to Western blot analysis. The blots were probed with HuR or GAPDH antibodies as indicated. **B**, autoradiographic images of the UV cross-linking experiments done with radioactive F-122 and F-421 transcripts and cytoplasmic extracts prepared from LNCaP cells transfected with scrambled, HuR, or AUF-1 siRNA duplexes. Twenty-four hours after transfection, cells were treated with PS-341 (500 nmol/L, 16 h), and the harvested cytoplasmic extracts were used for the analysis. UV cross-linking experiments were done as indicated in Materials and Methods. *Arrows*, molecular weights of protein standards and the HuR protein. **C**, quantitative real-time PCR analysis of RNA samples isolated from LNCaP cells transfected with scrambled or HuR siRNA. After 24 h of transfection, cells were treated with DMSO or PS-341 (100 nmol/L, 12 h) followed by actinomycin D (2  $\mu$ g/mL), and RNA was harvested at the times indicated. DR5 mRNA levels were normalized with endogenous GAPDH mRNA. Experiments were repeated in triplicate and the mean  $\pm$  the SD is plotted with the half-life of the mRNA (*solid horizontal line*). *Closed circles*, results from the scrambled siRNA; *open circles*, results from the cells treated with the siRNA for HuR. **D**, Western blot analysis was done for LNCaP cells transfected with Flag-HuR alone or along with a HA-ubiquitin cDNA construct. Twenty-four hours after transfection, cells were treated with PS-341 (500 nmol/L, 16 h) and the total extracts were prepared. The extracts were either loaded directly on SDS-PAGE or subjected to Flag (*lanes 5-10*) or HA (*lanes 11-14*) immunoprecipitation followed by either Flag (*lanes 1-8* and *11-14*) or HA (*lanes 9* and *10*) antibody Western blotting as indicated. One tenth of the total protein used for immunoprecipitation was loaded in *lanes 1* to *4*. *Right, brackets*, higher molecular weight bands consistent with multiubiquitinated HuR; *left, blunt arrows*, expression of Flag-HuR and its fragments.

fractionated via 10% SDS-PAGE. The binding of proteins to these 3'-UTR fragments are increased by PS-341 treatment of LNCaP cells, with the most prominent bands being  $\sim$ 36 and 45 kDa (Fig. 3B). Increased binding of these proteins to the F-1 fragment occurs in a time-dependent manner with maximal increase at  $\sim$ 17 h after PS-341 treatment (Fig. 3C). To examine the importance the F-1 and F-4 fragments to the regulation of mRNA stability, these fragments were cloned into the EGFP reporter and transfected into the LNCaP cells. By quantitative PCR, we find that treatment of cells

with PS-341 stabilized the mRNA containing each of these 3'-UTR fragments. This suggests that each of these fragments plays a role in regulating DR5 mRNA stability by this compound (Fig. 3D). It is possible that their additive effects would be similar to the entire 3'-UTR.

#### Analysis of Specific Protein Binding Sequences

Shorter deletion constructs of the F-1 and F-4 fragments were generated to select critical elements (see line diagrams in Fig. 4A and B) that bind mRNA-interacting proteins. The F-12 fragment had a protein binding pattern comparable

with F-1 (Fig. 4A). To ascertain the critical stabilizing elements, we further divided F-12 into two equal shorter transcripts of 75 bp: F-121 and F-122 (Fig. 4A). Autoradiographic images of the UV cross-linking experiments for F-121 and F-122 clearly indicate that the F-122, and not F-121 fragment, binds to cytoplasmic proteins; again, protein binding is increased by PS-341 treatment (Fig. 4A). Interestingly, F-122 fragment sequence analysis reveals two overlapping AU-rich nonamers (UUUAUUUAUUU-AUUU), which we have denoted F-122 AU-rich element. The F-4 region also strongly bound increased amounts of protein after PS-341 treatment. Analysis of smaller fragments (Fig. 4B) of this UTR fragment shows that the 71-bp section (denoted F-421) can bind these proteins. This fragment contains a significant U-rich stretch of nucleotides from 3,556 to 3,587 with the potential to interact with mRNA-binding proteins.

To identify whether the proteins binding fragments of the 3'-UTR were identical for both F-1 and F-4 regions, we did UV cross-linking experiments using either the 78-bp F-122 or F-421 as cold competitors (Fig. 4C). As shown in Fig. 4C, the F-421 fragment competed for protein binding to the F-1 fragment. Likewise, the F-122 fragment competed for protein binding to the F-4 fragment (Fig. 4D).

#### HuR Binds to F-1 and F-4 Regions of DR5 3'-UTR

To measure AU-rich binding proteins after PS-341 treatment, we prepared cytoplasmic and nuclear extracts from LNCaP cells treated with or without PS-341 for 18 h. These extracts were fractionated via 12% SDS-PAGE for subsequent Western blot analysis. Figure 5A shows an increase in cytoplasmic but not nuclear mRNA-binding protein including the AUF-1 isoforms, HuR, and hnRNP C1/C2. These proteins are increased 1.4-, 1.7-, and 4.8-fold respectively. In additional experiments (Fig. 6A for example), HuR increased between 2.2- and 2.4-fold. To evaluate whether specific proteins showed increased binding to the DR5 3'-UTR mRNA, we examined the proteins bound to this mRNA before and after PS-341 treatment. First, mRNA-binding proteins in the cytosol were immunoprecipitated using antibodies specific to HuR and TIAR (Fig. 5B); then, the extent of binding to the DR5 mRNA was evaluated by real-time PCR. Figure 5B shows a 5-fold increase in DR5 mRNA in the HuR samples immunoprecipitated from PS-341-treated LNCaP cells, whereas immunoprecipitation with TIAR did not bring down any DR5 transcript. To quantitate these changes more accurately, we did quantitative real-time PCR using DR5 primers (Fig. 5C). With this method, we report an 8-fold increase in HuR bound to DR5 mRNA after PS-341 treatment, but we observed no significant alteration in the binding of other AU-rich proteins, AUF-1, TIA-1, and TIAR, to the DR5 mRNA (Fig. 5C).

To assess whether the HuR protein interacts specifically with the F-1 and F-12 3'-UTR fragments, we examined the ability of antibodies specific to mRNA-binding proteins to immunoprecipitate radiolabeled F-1 and F-12 fragments. Autoradiographic images of the immunoprecipitated F-1 and F-12 transcripts (Fig. 5D) show that after PS-341

treatment HuR binding, but not TIAR binding, increased 3-fold to both F-1 and F-12 3'-UTR fragments. Together, these results confirm that the HuR binding protein is involved in DR5 mRNA stabilization after PS-341 treatment.

#### Knockdown of HuR Decreases DR5 mRNA Half-life

As shown in Fig. 6A, siRNA targeted at HuR markedly decreased HuR protein in control and PS-341-treated LNCaP cells but had no effect on GAPDH protein. This siRNA decreased the levels of HuR mRNA (data not shown). Figure 6B shows that knockdown of HuR using siRNA markedly decreases the binding of the 36-kDa protein induced by PS-341 to both F-122 and F-421 fragments of the 3'-UTR (Fig. 6B, lanes 3 and 4 and lanes 9 and 10). In comparison, knockdown of the AUF-1 protein (see Supplementary Fig. S1)<sup>1</sup> did not affect either the major 36- or 45-kDa bands seen on UV cross-linking (Fig. 6B, lanes 5 and 6 and lanes 11 and 12). HuR knockdown decreases the half-life of DR5 mRNA (Fig. 6C) from >8 to <4 h even after treatment with PS-341. Thus, HuR protein accounts for one of the major proteins bound to the 3'-UTR and knockdown of this protein negatively regulates the ability of PS-341 to stabilize DR5 mRNA.

#### PS-341-Driven Ubiquitination of HuR

To evaluate the possibility that PS-341 increased HuR protein by preventing its degradation by the proteasome, a HuR cDNA containing a Flag tag (a gift from J.A. Steitz) was transfected with or without a HA-ubiquitin plasmid. Western blot analysis of the extract with Flag antibody showed that the transfected HuR plasmid is expressed in LNCaP cells (Fig. 6D, 36-kDa band) and that treatment with PS-341 not only increased the amount of this protein but also increased HuR fragments (compare lanes 1 and 2, blunt arrows in Fig. 6D). When HA-ubiquitin is overexpressed along with HuR followed by the treatment with PS-341, HuR ubiquitination is markedly increased, and the 36-kDa band of HuR is shifted to a higher molecular weight band (Fig. 6D, lane 4). To further examine the possibility that HuR was ubiquitinated, this protein was immunoprecipitated with Flag beads and then Western blotted with a Flag antibody. Only in cells transfected with Flag HuR and HA-ubiquitin did PS-341 treatment induce higher molecular weight bands of HuR protein (Fig. 6D, lane 8, bracket). If this Western blot is then stripped and probed with a HA antibody, the high molecular weight bands recognized by this antibody (Fig. 6D, lane 10) are shown to contain ubiquitin. Similarly, if the transfected proteins were immunoprecipitated with HA antibody and then Western blotted with Flag antibody, a high molecular weight band was seen only when doubly transfected cells were treated with PS-341 (Fig. 6D, lane 14). Thus, it is possible that increases in HuR induced by PS-341 treatment could be secondary to the inhibition of the degradation of this protein.

## Discussion

Here, we provide data to support a novel mechanism underlying the elevation of DR5 by PS-341. PS-341

treatment increases DR5 mRNA by stabilizing the mRNA half-life from 4 to ~10 h. Our results suggest that this increase in stability is secondary to binding of specific proteins to the DR5 3'-UTR. First, we showed that transferring the 3'-UTR of DR5 to a heterologous mRNA, EGFP, allows this transcript stabilization via PS-341 treatment of transfected LNCaP cells. Second, we show that PS-341 increases protein binding to fragments F-1 and F-4 of the DR5 3'-UTR that contain A/U-rich sequences. Third, we provide evidence that PS-341 treatment increases cytoplasmic multiple mRNA-binding proteins, including HuR, which is known to stabilize mRNAs. Fourth, we show that PS-341 treatment increased HuR protein bound to the DR5 3'-UTR. Finally, we provide data to suggest that protein knockdown with siRNA decreases the ability of PS-341 to prolong the half-life of this mRNA.

Our experiments show that PS-341 treatment has the potential to block the degradation of HuR and increases its ubiquitination leading to elevated HuR. We have not ruled out the possibility that increases in HuR protein in the cytoplasm arise from inhibition of various signal transduction pathways, that is, AMP-activated protein kinase (41, 42) that regulate transport of this protein from the nucleus to the cytosol. We have focused our studies on LNCaP cells, because in this cell type PS-341 markedly enhances TRAIL-induced tumor cell killing by elevating DR5 (12). However, we show that the ability of PS-341 to prolong mRNA half-life is clearly cell type specific; this does not occur with either PC-3 or DU145 human prostate cancer cell lines. It is possible that differences among these cells are secondary to the availability of proteasome subunits. Recent experiments show that the proteasome expression levels and subunit composition in B-cell lines influence response to proteasome inhibition (43).

It is possible in the absence of PS-341 treatment that negative regulators of mRNA stability bind and regulate the DR5 3'-UTR and that changes in HuR protein levels lead to the replacement of these proteins on the mRNA with stabilization. We have observed that overexpression of tristetraprolin in HeLa cells suppresses the expression of DR5 mRNA.<sup>2</sup> However, we have not identified significant tristetraprolin bound to DR5 mRNA in LNCaP cells. The potential absence of identified mRNA decay proteins bound to the 3'-UTR may be due to the fact that the binding of these proteins stimulates the rapid degradation of the DR5 mRNA. Thus, in LNCaP cells not treated with PS-341, attempting to immunoprecipitate destabilizing proteins bound to the DR5 mRNA may be technically difficult (44).

The observation that the HuR protein and AUF-1 are both increased by PS-341 treatment complements the observation that AUF-1 is also ubiquitinated and the levels of this protein are controlled by the proteasome (45–48). However, the AUF-1 family of four proteins is complicated, with

p37 and p40 isoforms being ubiquitinated and having mRNA destabilizing activity (45–48). When evaluating the stability of mRNAs that contain binding sites for both HuR and AUF-1 proteins (44), the stability or degradation of a specific mRNA was determined by the amount of each protein present in the cytoplasm. Using siRNA targeted at all four AUF-1 isoforms, we did not find major changes in the proteins bound to the DR5 3'-UTR, suggesting that this protein alone does not play a role in regulating the DR5 mRNA. To evaluate the importance of HuR levels alone on TRAIL plus PS-341 killing, we knocked down HuR with siRNA and then treated LNCaP cells with each agent alone or in combination. Although knockdown of HuR did significantly increase cell viability, the change in the number of viable cells was not large (Supplementary Fig. S2).<sup>1</sup> Possible reasons to explain this could be that both the 36-kDa protein HuR and the unknown 45-kDa protein may be coordinately regulating the posttranscriptional process. Both proteins may need to be simultaneously knocked down to see a major effect. Alternatively, PS-341 has multiple other effects, including elevating levels of BH3 proteins Noxa, Bik, and Bim (10, 49), which could be as important to apoptosis as increases in DR5 levels.

In summary, our results suggest a novel mechanism, mRNA stabilization, by which the proteasome inhibitor PS-341 regulates DR5 mRNA and its protein. This work further clarifies the mechanism by which PS-341 enhances sensitivity of cancer cells to the apoptotic agent TRAIL. Modulating the amount or activity of mRNA-binding proteins has great promise for enhancing cancer chemotherapy.

## Disclosure of Potential Conflicts of Interest

No potential conflicts of interest were disclosed.

## Acknowledgments

We thank Dr. Joan A. Steitz (Howard Hughes Medical Institute, Yale University) for the gift of Flag-HuR plasmid, Dr. Ann-Bin Shyu (University of Texas Health Science Center) for the gift of the rat-GAPDH plasmid that was used to normalize all quantitative PCR, Dr. Baby G. Tholanikunnel (Medical University of South Carolina) for the Sh-RNA plasmid for HuR in the initial part of the study, the Millennium Corp. for providing PS-341, and the Statistical Core of the Hollings Cancer Center, headed by Dr. Elizabeth Garrett-Mayer, which carried out the analysis of these data.

## References

1. Chaudhari BR, Murphy RF, Agrawal DK. Following the TRAIL to apoptosis. *Immunol Res* 2006;35:249–62.
2. Bremer E, van Dam G, Kroesen BJ, de Leij L, Helfrich W. Targeted induction of apoptosis for cancer therapy: current progress and prospects. *Trends Mol Med* 2006;12:382–93.
3. Clarke N, Nebbioso A, Altucci L, Gronemeyer H. TRAIL: at the center of drugable anti-tumor pathways. *Cell Cycle* 2005;4:914–8.
4. Marini P, Denzinger S, Schiller D, et al. Combined treatment of colorectal tumours with agonistic TRAIL receptor antibodies HGS-ETR1 and HGS-ETR2 and radiotherapy: enhanced effects *in vitro* and dose-dependent growth delay *in vivo*. *Oncogene* 2006;25:5145–54.
5. Pukac L, Kanakaraj P, Humphreys R, et al. HGS-ETR1, a fully human TRAIL-receptor 1 monoclonal antibody, induces cell death in multiple tumour types *in vitro* and *in vivo*. *Br J Cancer* 2005;92:1430–41.
6. Zeng Y, Wu XX, Fiscella M, et al. Monoclonal antibody to tumor necrosis factor-related apoptosis-inducing ligand receptor 2 (TRAIL-R2)

<sup>2</sup> D. Dixon et al., University of South Carolina, unpublished data.

- induces apoptosis in primary renal cell carcinoma cells *in vitro* and inhibits tumor growth *in vivo*. *Int J Oncol* 2006;28:421–30.
7. Adams J, Palombella VJ, Elliott PJ. Proteasome inhibition: a new strategy in cancer treatment. *Cancer Res* 2000;18:109–21.
  8. Sayers TJ, Brooks AD, Koh CY, et al. The proteasome inhibitor PS-341 sensitizes neoplastic cells to TRAIL-mediated apoptosis by reducing levels of c-FLIP. *Blood* 2003;102:303–10.
  9. Nencioni A, Wille L, Dal Bello G, et al. Cooperative cytotoxicity of proteasome inhibitors and tumor necrosis factor-related apoptosis-inducing ligand in chemoresistant Bcl-2-overexpressing cells. *Clin Cancer Res* 2005;11:4259–65.
  10. Nikrad M, Johnson T, Puthalalath H, Coultas L, Adams J, Kraft AS. The proteasome inhibitor bortezomib sensitizes cells to killing by death receptor ligand TRAIL via BH3-only proteins Bik and Bim. *Mol Cancer Ther* 2005;4:443–9.
  11. Zhu H, Guo W, Zhang L, et al. Proteasome inhibitors-mediated TRAIL resensitization and Bik accumulation. *Cancer Biol Ther* 2005;4:781–6.
  12. Johnson TR, Stone K, Nikrad M, et al. The proteasome inhibitor PS-341 overcomes TRAIL resistance in Bax and caspase 9-negative or Bcl-xL overexpressing cells. *Oncogene* 2003;22:4953–63.
  13. Mitsiades N, Mitsiades CS, Poulaki V, et al. Molecular sequelae of proteasome inhibition in human multiple myeloma cells. *Proc Natl Acad Sci U S A* 2002;99:14374–9.
  14. Fleming JA, Lightcap ES, Sadis S, Thoroddsen V, Bulawa CE, Blackman RK. Complementary whole-genome technologies reveal the cellular response to proteasome inhibition by PS-341. *Proc Natl Acad Sci U S A* 2002;99:1461–6.
  15. Obeng EA, Carlson LM, Gutman DM, Harrington WJ, Jr., Lee KP, Boise LH. Proteasome inhibitors induce a terminal unfolded protein response in multiple myeloma cells. *Blood* 2006;107:4907–16.
  16. Fribley A, Wang CY. Proteasome inhibitor induces apoptosis through induction of endoplasmic reticulum stress. *Cancer Biol Ther* 2006;5:745–8.
  17. Fribley A, Zeng Q, Wang CY. Proteasome inhibitor PS-341 induces apoptosis through induction of endoplasmic reticulum stress-reactive oxygen species in head and neck squamous cell carcinoma cells. *Mol Cell Biol* 2004;24:9695–704.
  18. Yoshida T, Shiraishi T, Nakata S, et al. Proteasome inhibitor MG132 induces death receptor 5 through CCAAT/enhancer-binding protein homologous protein. *Cancer Res* 2005;65:5662–7.
  19. Yamaguchi H, Wang HG. CHOP is involved in endoplasmic reticulum stress-induced apoptosis by enhancing DR5 expression in human carcinoma cells. *J Biol Chem* 2004;279:45495–502.
  20. Wu GS, Kim K, el-Deiry WS. KILLER/DR5, a novel DNA-damage inducible death receptor gene, links the p53-tumor suppressor to caspase activation and apoptotic death. *Adv Exp Med Biol* 2000;465:143–51.
  21. Takimoto R, El-Deiry WS. Wild-type p53 transactivates the KILLER/DR5 gene through an intronic sequence-specific DNA-binding site. *Oncogene* 2000;19:1735–43.
  22. Shetty S, Graham BA, Brown JG, et al. Transcription factor NF- $\kappa$ B differentially regulates death receptor 5 expression involving histone deacetylase 1. *Mol Cell Biol* 2005;25:5404–16.
  23. Carballo E, Lai WS, Blakeshear PJ. Evidence that tristetraprolin is a physiological regulator of granulocyte-macrophage colony-stimulating factor messenger RNA deadenylation and stability. *Blood* 2000;95:1891–9.
  24. Du G, Yonekubo J, Zeng Y, Osisami M, Frohman MA. Design of expression vectors for RNA interference based on miRNAs and RNA splicing. *FEBS J* 2006;273:5421–7.
  25. Hitti E, Iakovleva T, Brook M, et al. Mitogen-activated protein kinase-activated protein kinase 2 regulates tumor necrosis factor mRNA stability and translation mainly by altering tristetraprolin expression, stability, and binding to adenine/uridine-rich element. *Mol Cell Biol* 2006;26:2399–407.
  26. Laflam PF, Haraguchi S, Garin EH. Cytokine mRNA profile in lipoid nephrosis: evidence for increased IL-8 mRNA stability. *Nephron* 2002;91:620–6.
  27. Ogilvie RL, Abelson M, Hau HH, Vlasova I, Blakeshear PJ, Bohjanen PR. Tristetraprolin down-regulates IL-2 gene expression through AU-rich element-mediated mRNA decay. *J Immunol* 2005;174:953–61.
  28. Patil C, Zhu X, Rossa C, Jr., Kim YJ, Kirkwood KL. p38 MAPK regulates IL-1 $\beta$  induced IL-6 expression through mRNA stability in osteoblasts. *Immunol Invest* 2004;33:213–33.
  29. Chang TC, Yamashita A, Chen CY, et al. UNR, a new partner of poly(A)-binding protein, plays a key role in translationally coupled mRNA turnover mediated by the c-fos major coding-region determinant. *Genes Dev* 2004;18:2010–23.
  30. Lai WS, Carballo E, Strum JR, Kennington EA, Phillips RS, Blakeshear PJ. Evidence that tristetraprolin binds to AU-rich elements and promotes the deadenylation and destabilization of tumor necrosis factor  $\alpha$  mRNA. *Mol Cell Biol* 1999;19:4311–23.
  31. Cao H, Tuttle JS, Blakeshear PJ. Immunological characterization of tristetraprolin as a low abundance, inducible, stable cytosolic protein. *J Biol Chem* 2004;279:21489–99.
  32. Stoecklin G, Colombi M, Raineri I, et al. Functional cloning of BRF1, a regulator of ARE-dependent mRNA turnover. *EMBO J* 2002;21:4709–18.
  33. Yamasaki S, Stoecklin G, Kedersha N, Simarro M, Anderson P. T-cell intracellular antigen-1 (TIA-1)-induced translational silencing promotes the decay of selected mRNAs. *J Biol Chem* 2007;282:30070–7.
  34. Fan XC, Steitz JA. Overexpression of HuR, a nuclear-cytoplasmic shuttling protein, increases the *in vivo* stability of ARE-containing mRNAs. *EMBO J* 1998;17:3448–60.
  35. Chen CY, Xu N, Shyu AB. Highly selective actions of HuR in antagonizing AU-rich element-mediated mRNA destabilization. *Mol Cell Biol* 2002;22:7268–78.
  36. Wilson GM, Lu J, Sutphen K, Sun Y, Huynh Y, Brewer G. Regulation of A + U-rich element-directed mRNA turnover involving reversible phosphorylation of AUF1. *J Biol Chem* 2003;278:33029–38.
  37. Zhang XY, Zhang XD, Borrow JM, Nguyen T, Hersey P. Translational control of tumor necrosis factor-related apoptosis-inducing ligand death receptor expression in melanoma cells. *J Biol Chem* 2004;279:10606–14.
  38. Wang P, Song JH, Song DK, Zhang J, Hao C. Role of death receptor and mitochondrial pathways in conventional chemotherapy drug induction of apoptosis. *Cell Signal* 2006;18:1528–35.
  39. Ford LP, Wilusz J. An *in vitro* system using HeLa cytoplasmic extracts that reproduces regulated mRNA stability. *Methods* 1999;17:21–7.
  40. Tenenbaum SA, Lager PJ, Carson CC, Keene JD. Ribonomics: identifying mRNA subsets in mRNP complexes using antibodies to RNA-binding proteins and genomic arrays. *Methods* 2002;26:191–8.
  41. Galban S, Martindale JL, Mazan-Mamczarz K, et al. Influence of the RNA-binding protein HuR in pVHL-regulated p53 expression in renal carcinoma cells. *Mol Cell Biol* 2003;23:7083–95.
  42. Wang W, Yang X, Lopez de Silanes I, Carling D, Gorospe M. Increased AMP:ATP ratio and AMP-activated protein kinase activity during cellular senescence linked to reduced HuR function. *J Biol Chem* 2003;278:27016–23.
  43. Busse A, Kraus M, Na IK, et al. Sensitivity of tumor cells to proteasome inhibitors is associated with expression levels and composition of proteasome subunits. *Cancer* 2008;12:657–70.
  44. Lal A, Mazan-Mamczarz K, Kawai T, Yang X, Martindale JL, Gorospe M. Concurrent versus individual binding of HuR and AUF1 to common labile target mRNAs. *EMBO J* 2004;23:3092–102.
  45. Laroia G, Schneider RJ. Alternate exon insertion controls selective ubiquitination and degradation of different AUF1 protein isoforms. *Nucleic Acids Res* 2002;30:3052–8.
  46. Laroia G, Cuesta R, Brewer G, Schneider RJ. Control of mRNA decay by heat shock-ubiquitin-proteasome pathway. *Science* 1999;284:499–502.
  47. Laroia G, Sarkar B, Schneider RJ. Ubiquitin-dependent mechanism regulates rapid turnover of AU-rich cytokine mRNAs. *Proc Natl Acad Sci U S A* 2002;99:1842–6.
  48. Raineri I, Wegmueller D, Gross B, Certa U, Moroni C. Roles of AUF1 isoforms, HuR and BRF1 in ARE-dependent mRNA turnover studied by RNA interference. *Nucleic Acids Res* 2004;32:1279–88.
  49. Gomez-Bougie P, Willeme-Toumi S, Menoret E, et al. Noxa up-regulation and Mcl-1 cleavage are associated to apoptosis induction by bortezomib in multiple myeloma. *Cancer Res* 2007;67:5418–24.

# Molecular Cancer Therapeutics

## Proteasome inhibitor PS-341 (VELCADE) induces stabilization of the TRAIL receptor DR5 mRNA through the 3' -untranslated region

Karthikeyan Kandasamy and Andrew S. Kraft

*Mol Cancer Ther* 2008;7:1091-1100.

<b>Updated version</b>	Access the most recent version of this article at: <a href="http://mct.aacrjournals.org/content/7/5/1091">http://mct.aacrjournals.org/content/7/5/1091</a>
<b>Supplementary Material</b>	Access the most recent supplemental material at: <a href="http://mct.aacrjournals.org/content/suppl/2008/07/18/7.5.1091.DC1">http://mct.aacrjournals.org/content/suppl/2008/07/18/7.5.1091.DC1</a>

<b>Cited articles</b>	This article cites 49 articles, 28 of which you can access for free at: <a href="http://mct.aacrjournals.org/content/7/5/1091.full#ref-list-1">http://mct.aacrjournals.org/content/7/5/1091.full#ref-list-1</a>
<b>Citing articles</b>	This article has been cited by 4 HighWire-hosted articles. Access the articles at: <a href="http://mct.aacrjournals.org/content/7/5/1091.full#related-urls">http://mct.aacrjournals.org/content/7/5/1091.full#related-urls</a>

<b>E-mail alerts</b>	<a href="#">Sign up to receive free email-alerts</a> related to this article or journal.
<b>Reprints and Subscriptions</b>	To order reprints of this article or to subscribe to the journal, contact the AACR Publications Department at <a href="mailto:pubs@aacr.org">pubs@aacr.org</a> .
<b>Permissions</b>	To request permission to re-use all or part of this article, use this link <a href="http://mct.aacrjournals.org/content/7/5/1091">http://mct.aacrjournals.org/content/7/5/1091</a> . Click on "Request Permissions" which will take you to the Copyright Clearance Center's (CCC) Rightslink site.